CRISPR/Cas9-induced saturated mutagenesis identifies *Rad51* haplotype as a marker of PARP inhibitor sensitivity in breast cancer

HUA YANG, YANING WEI, QIAN ZHANG, YANG YANG, XUEBING BI, LIN YANG, NA XIAO, AIMIN ZANG, LILI REN and XIAOLI LI

Department of Medical Oncology, Affiliated Hospital of Hebei University, Hebei Key Laboratory of Cancer Radiotherapy and Chemotherapy, Baoding, Hebei 071000, P.R. China

Received January 28, 2022; Accepted May 16, 2022

DOI: 10.3892/mmr.2022.12774

Abstract. Breast cancer treatment with poly(ADP-ribose)polymerase (PARP) inhibitors is currently limited to cells defective in the homologous recombination repair (HRR) pathway. The chemical inhibition of many HRR deficiency genes may sensitize cancer cells to PARP inhibitors. In the present study, *Rad51*, a central player in the HRR pathway, was selected to explore additional low variation and highly representative markers for PARP inhibitor activity. A CRISPR/Cas9-based saturated mutation approach for the *Rad51* WALKER domain was used to evaluate the sensitivity of the PARP inhibitor olaparib. Five amino acid mutation sites were identified in olaparib-resistant cells. Two *Rad51* haplotypes were assembled from the mutations, and may represent useful pharmacogenomic markers of PARP inhibitor sensitivity.

Introduction

The *Brca1* and *Brca2* genes play central roles in homologous recombination repair (HRR) (1,2). Mutations of *Brca1* and *Brca2* are normally observed in many familial cases; for example, mutations in rare high-penetrating breast cancer account for 16-25% of the inherited cancer type (3). Given the high prevalence of polymorphisms of these two genes, some agents are unable to target the translated proteins and poly(ADP-ribose) polymerase (PARP) provides an alternative approach by targeting the HRR pathway (4). In recent years, several PARP inhibitors have been approved by the US Federal Drug Administration (FDA) as effective chemotherapy reagents for various cancers with mutations in *Brca1* and *Brca2* (5). Acting as substitutes for *Brca1*, a series of genes have been identified as DNA repair regulators, such as *Nbn*, *Fancd2*, *Rad51*, *Lig3*, *Rad51C*, *Rad21* and *Esco1* (6). All of these genes and related pathways are closely linked to the HRR pathway and the response to PARP inhibitors; however, only 40% of patients who receive PARP inhibitor treatment respond effectively. Although platinum sensitivity has been suggested as a hallmark of response to PARP inhibitors, patients with platinum-resistant disease still respond to Olaparib (1). Therefore, a thorough understanding of the genetic determinants that contribute to the sensitivity of PARP inhibitors will increase their clinical utility.

A central player in the HRR pathway is the RAD51 recombinase that binds to single-stranded DNA at break sites (7). RAD51 can bind to the break sites participating with BRCA2 and five other paralogs, namely, RAD51B, RAD51C, RAD51D, XRCC2, and XRCC3 (8). Cruz *et al* regarded Rad51 nuclear foci as an indicator of PARP inhibitor resistance in breast or ovarian cancer with germline *Brca1*/2 (gBRCA) mutations (9) while others have considered them regulators of sensitivity to PARP inhibitors beyond *Brca1*/2-related cancers (10). Olaparib-RAD51 inhibitor conjugates have also been reported to break resistance mechanisms to olaparib treatment in triple-negative breast cancer cells regardless of BRCA status (11). RAD51 nuclear foci formation is also closely correlated with TOPBP1-dependent phosphorylation and contributes to PARP inhibitor resistance (12). Some mutation signatures of *Rad51* and the participating proteins are closely correlated with the resistance to PARP inhibitors, although other *Rad51* paralogs and participating protein mutants are also sensitive to PARP inhibitors (13-15). Therefore, more studies are necessary to identify the genetic polymorphisms of *Rad51* that may contribute to sensitivity to the PARP inhibitor.

Clustered regular interval short palindromic repeat (CRISPR)-directed Cas9-mediated endonuclease activity has been described as an effective strategy to induce saturated

Correspondence to: Dr Lili Ren or Dr Xiaoli Li, Department of Medical Oncology, Affiliated Hospital of Hebei University, Hebei Key Laboratory of Cancer Radiotherapy and Chemotherapy, 212 Yuhua East Road, Baoding, Hebei 071000, P.R. China
E-mail: hbuoncology@126.com
E-mail: xiaolilihbu@126.com

Abbreviations: CRISPR, clustered regular interval short palindromic repeats; HDR, homology-directed repair; HRR, homologous recombination repair; OTS, off-target sites; PAM, protospacer adjacent motif; PARP, poly(ADP-ribose)polymerase

Key words: PARP inhibitor, CRISPR/Cas9, *Rad51*, haplotype, breast cancer

mutations in a specific genome locus, and mutations have been identified that contribute to drug resistance (16,17). Compared to a random screening strategy, a site-specific saturated mutation approach has been more effective and specific in discovering drug resistance mutations (16-18). Moreover, mutations near specific loci are more easily inherited as haplotypes. Compared to individual single nucleotide polymorphism (SNP) sites, the haplotype represents a more clinically effective biomarker (19).

An α/β ATPase core domain similar to those present in helicases is also found in the RAD51 protein. WALKER A and B motifs in the α/β ATPase domain are key to ATP binding and hydrolysis (20,21). HRR-related protein complex assembly and DNA strand exchange activity are coupled to the binding and hydrolysis of ATP by RAD51 (22). Therefore the WALKER A and B motifs signaling between binding sites for DNA and nucleotide ligands are critical for RAD51 recombination activity. WALKER A and B domains of *Rad51* have been identified as key players in the HRR pathway (23). Previous studies have also presented series mutations which are requirements for the WALKER A and B motifs for *Rad51*D function in response to DNA damage (22,24). In terms of technical feasibility, the relatively short length of WALKER A and B motifs (8 and 5 amino residues, respectively) is within the limit of saturated mutational library content and suitable for saturated mutagenesis. All of the above evidence indicates that investigation of all the potential mutations in the WALKER domain is valuable and feasible. Identification of these functional mutations and the highly correlated variations may lead to a high throughput approach for the selection of pharmacogenomics targets. This study aimed to identify olaparib sensitivity-related mutations of *Rad51* WALKER domain which were induced by a CRISPR/Cas9-based saturated mutational library in breast cancer cells, and to assess their clinical value. We selected *Rad51* because previous resistance to PARP inhibitors is associated with the number of RAD51 nuclear foci (9) and hazard ratio (HR) efficiency mutations of *Rad51* and its paralog gene are observed in the WALKER domain (13), which is highly conserved in this gene family. To identify clinically valuable mutations, we chose to target an exon in a clinically relevant domain in which known mutations are associated with poor outcomes. Previous molecular studies of three nonsense mutations located in the WALKER motif greatly contributed to HRR efficiency (15). We hypothesized that saturation genome editing would result in a wide range of outcomes.

Materials and methods

Cell line sensitivity to olaparib (Pilot study). The five candidate breast cancer cell lines (HCC1599, BT-549, Hs578T, MDA-MB-231 and MDA-MB-453) were seeded in 6-well plates (4,000 cells/well) and incubated in Dulbecco's modified Eagle's medium (DMEM) or Roswell Park Memorial Institute-1640 (RPMI-1640) medium with 10% fetal bovine serum (FBS). Drug-containing medium (50 μM olaparib) was refreshed weekly (25). A total of 10^6 cells were digested with trypsin after 24 h of culturing, followed by centrifugation at 110 x g for 5 min, and then cleaned twice and centrifuged at 110 x g for a further 5 min. The collected cells were fixed with 1 ml ethanol at 4˚C overnight. Then, 100 μl of RNase A (Solarbio) was added to incubate the cells at 37˚C in the dark for 30 min. Propidium iodide (PI) (50 μl) was then added. After further incubation in the dark for 1 h at 25˚C, the cells were detected by flow cytometry (Becton, Dickinson and Company). Finally, the flow cytometric data were analyzed using FlowJo software version 10 (Tree Star, Inc.). All the cell culture media and related reagent were purchased from Thermo Fisher Scientific, Inc.

Construction of the Cas9 and sgRNA vectors. Five sgRNAs (sgRNA1-1, sgRNA1-2, sgRNA2-1, sgRNA2-2, and sgRNA2-3) were selected in the WALKER A and B *Rad51* domains using an online predictor tool CCTOP (http://crispr.cos.uni-heidelberg.de) (26). The sgRNAs were then cloned into a human codon-optimized *Streptococcus* (*S. pyogenous*) Cas9-sgRNA vector (pX330-U6-Chimeric_BB-CBh-hSpCas9; Addgene plasmid #42230, Addgene). There were three reasons to choose this cell line. i) The function of *Rad51* is closely linked with *Brca1*/2 whose gene products act upstream of *Rad51* in HR (27). In order to eliminate interference influence of the *BRCA* gene status, the candidate cell lines do not carry the *Brca1/2* mutations, as indicated by the American Type Culture Collection (ATCC) document (characterization data and other information relating to this material are available at www.atcc.org). ii) Given the high cost and off-target ratio of CRISPR/Cas9-based experiments, it is sensible to choose cells which have been used in similar experiments, as is the case for BT-549 cells (28). iii) Cells should have high sensitivity to olaparib, and in the pilot study (described above; see also Results and Fig. S1) BT-549 cells showed the highest apoptosis ratio induced by olaparib. Thus, BT-549 cells were selected as the *in vitro* cell model for this study. Five sgRNAs (the top sgRNAs scored by CCTOP) for four targeted sites were selected for each predicted locus and were cloned into the CRISPR/Cas9 vector (Table I). The constructed vector was packaged in lentiviruses, which were then transfected into BT-549 cells. One microgram of the Cas9-sgRNA vector was used to transfect BT-549 cells by electroporation. Briefly, the $2x10^6$ cells with Cas9-sgRNA vector complex per reaction were used for electroporation following the standard instruction of the Neon™ Transfection System (cat. no. MPK10025, Thermo Fisher Scientific, Inc.). The program (1600 V/10 msec/3 pulses) was adopted for electroporation at room temperature. After the electroporation, the cells were immediately transferred to a 24-well plate containing 0.5 ml of pre-warmed culture medium for recovery at 37˚C. After 48 h of recovery, genomic DNA was extracted for polymerase chain reaction (PCR). The cleavage efficiency was evaluated using the T7E1 cleavage assay (NEB) as described previously (27). Potential off-target sites (OTS) were predicted using the CCTOP online prediction tool, amplified from the genomic DNA of the *Rad51* KO BT_549, and sequenced. Bulk PCR products can also be sequenced using a next generation sequencing (NGS) approach followed by software analysis. The off-target ratios were indicated by the off-target/total reads count. Potential off-target sites were predicted using the CCTOP online predicting tool and then amplified from the genomic DNA extracted from *Rad51*-knockout (KO) BT-549 cells. The

Table I. sgRNAs for the WALKER domain A and B.

Name	Target domain	DNA strand	Sequence (5'-3')
sgRNA-1-1	WALKER domain A	(+)	GGATCTATCACAGAAATGTTTGG
sgRNA-1-2	WALKER domain A	(-)	AGCTAGCGTATGACAGATCTGGG
sgRNA-2-1	WALKER domain B	(+)	AAGGGACCAGAATCTGACACAGG
sgRNA-2-2	WALKER domain B	(-)	GTCTGTTCTGTAAAGGGCGGTGG
sgRNA-2-3	WALKER domain B	(+)	AGAACAGACTACTCGGGTCGAGG

Table II. List of primer sequences used for the HDR donor library construction.

Name	Forward primer (5'-3')	Reverse primer (5'-3')
WALKERA-1	ACAGGTGCCCATCACCAGTTCC	CTTGGGAGGCCAAGGTGGGT
WALKERA-2	TTGAAACAGGGTCTCACTGTG	TTACGCCTATAATTCCAGCAC
WALKERB-1	TGACACTCTTGCTTTGTAG	TGCATGGGCGATGATATTTCC
WALKERB-2	TGCCTCAGATGTTAGTACTGT	ATGTCTTCACAGTTAATATGA
WALKERB-3	AAACATCTATATACAGGCCGG	ACAGTAGCTTTAACAGGGCT

HDR, HDR, homology-directed repair.

variants were identified by sequence alignment. The primers used to amplify the OTS are listed in Table SI.

Western blot analysis. Total proteins were extracted by using RIPA Lysis Buffer (cat. no. P0013E; Beyotime Institute of Biotechnology). The BCA Protein Assay kit (cat. no. P0012S; Beyotime Institute of Biotechnology) was used to determine the concentration of protein extracted from each sample. SDS-PAGE (on 10% gel) was then adopted to isolate the protein (40 μg) from each sample after which samples were removed to a polyvinylidene fluoride (PVDF) membrane. The film was then blocked for 1 h in 5% nonfat milk at 4˚C. The membrane was then incubated in primary monoclonal and secondary antibodies (all from Abcam) against GAPDH (cat. no. ab8245, dilution 1:1,000), pro-caspase-3 (cat. no. ab179517, dilution 1:1,000), cleaved caspase 3 (cat. no. ab2302, dilution 1:500), Bcl-2 (cat. no. ab32124, dilution 1:500), Bax (cat. no. ab205718, dilution 1:500) for 2 h at 4˚C. The secondary antibodies were anti-rabbit (cat. no. ab205718, dilution 1:1,000) conjugated with horseradish peroxidase for 1 h at room temperature. Lastly, the signals were visualized using an enhanced ECL Western blotting kit (Abcam), and the optical density of each band was analyzed by Gel-Pro-Analyze software (version 4.5; Media Cybernetics, Inc.).

Homology-directed repair (HDR) library construction. Given the high number of variants in the homology-directed repair (HDR)-edited loci, evaluation of each variant in gDNA from a population of unedited cells would require a large amount of sequencing and sufficient cells. To improve the HDR efficiency, we introduced mutations between the protospacer adjacent motif (PAM) and the protospacer sequences, which would prevent Cas9 from recutting HDR-edited genomes. Based on a previous study, we designed PCR-selective sites in the sequence (17). An HDR library containing all 6,859 possible DNA residues substituted at positions +37 to +40 and +52 to 55 of *Rad51* exon 5 and +17 to +19 of exon 8 was constructed using series of oligonucleotide. The oligonucleotide was then cloned through the In-Fusion reaction (Clontech; Takara Bio USA) into a pUC19 vector containing a preinserted 1000 bp fragment as homologous arms (Table II). Finally, the amplification products were purified and ligated in a pRNDM vector in frame as described above (28).

Lentiviral particle production. Thirteen million 293(T) cells (ATCC) were cultured in a 15-cm dish with 15 ml Opti-MEM (Thermo Fisher Scientific, Inc.) in a 5% CO_2 incubator at 37˚C with 95% humidity. The third-generation packaging system was used in this experiment. Transfection of 16 μg genome-editing vectors (donor template library, lenti-Cas9) with 16 μg packaging plasmid psPAX2 and 6 μg envelope plasmid pMD2.G (Thermo Fisher Scientific, Inc.) were mixed in 1 ml Opti-MEM. About 76 μl of 1 mg/ml polyethylenimine (Polysciences Inc.) was mixed with the plasmids in 1 ml Opti-MEM for 15 min at room temperature. The DNA/PEI mixture was then added to the 293(T) cells in Opti-MEM. Forty-eight hours after transfection, cell culture medium was collected and centrifuged at 200 x g at 4˚C for 10 min. The supernatant was then filtered through Φ 0.45-μm low-protein binding HV/PVDF membrane (Merck KGaA). The viral dose (multiplicity of infection ≈0.5) was identified and used to infect the cells. Aliquots of the supernatant containing viral particles were stored at -80˚C until required.

BT-549 cell culture condition. The human breast cell line BT-549 (ATCC) was used as the cell model, as explained above. All cell lines were subjected to confirmation of cell line identity. Cells were cultured in a medium composed

Table III. List of primer sequences used for selective PCR.

Name	Forward primer (5'-3')	Reverse primer (5'-3')
WALKERA-1	ATCTATCACAGAA**GCCGGAT**G	TATTAACAGCTATAAGATT
WALKERA-2	TAAGCTTCCTAAAGTGCT	GCTAGCGTATGA**CATCAGCT**G
WALKERB-1	GGACCAGAATCT**GAGACTC**G	TCTCTCTTCTTCCTAAGAGCT
WALKERB-2	TCCGGAGGCTGAAGCAGGAG	CTGTTCTGTAAA**TGACACT**G
WALKERB-3	ACTGCACTCCAGCCTGGGCG	C**AGCTCTG**AAAGCTCACCTCGA

Bold typeface indicates the 7-bp selective PCR site.

of 10% FBS and 90% RPMI-1640 medium in a 5% CO_2 incubator at 37˚C with 95% humidity. Cells were harvested at 80% confluence and were used for subsequent experiments. All media were supplemented with 100 U/ml penicillin and 100 μg/ml streptomycin (Thermo Fisher Scientific, Inc.).

Drug treatment, library construction, and next-generation sequencing. Construction of the donor libraries was as described in a previous study (29). Cell cultures were co-infected with equivalent amounts of amplified lentiviral library and CRISPR/Cas9-sg *Rad51*. Cells were seeded in 100-mm dishes with $3x10^6$ cells per dish. Puromycin (Merck KGaA) was added into the selection media after lentiviral infection and cultured at 2 μg/ml for one day. After selection, the surviving cells were pooled and used for amplification culture for 7 days. During the amplification culture, selection medium (containing 2 μg/ml puromycin) was replaced every 2-3 days. The surviving cells were then split into three individual groups that were treated with DMSO (Merck KGaA), 5 or 10 μM olaparib for 1 week. For each treatment, $1x10^7$ cells per replicate were used. Genomic DNA was extracted and real-time PCR (RT-PCR) was performed using the specific primers listed in Table III. PCR product was separated using agarose gel electrophoresis, then an QIAquick Gel Extraction Kit (cat. no. 28704, Qiagen, Inc.) was used to isolate DNA. The concentration of the DNA was quantified using a Qubit 2.0 Fluorometer (Thermo Fisher Scientific, Inc.). DNA quality was determined by measuring 260/280 and 230/260 absorbance ratios on a spectrophotometer (Nanodrop ND-1000, Peqlab Biotechnologie). The DNA integrity number was determined using the Lab-on-a-Chip-System Bio-analyzer 2100 (Agilent Technologies, Inc.). The PCR products were used to prepare the NGS library. The library for sequencing was constructed using the NEB Next Ultra II DNA Library Prep Kit (cat. no. NEB#E7645L, NEB) in line with the manufacturer's instructions. The average insert fragment in the library (approximately 292 bp) was measured and controlled using the Bioanalyzer 2100 (Agilent Technologies, Inc.). The final library concentration was measured and adjusted to approximately 10 ng/μl using the Qubit 2.0 Fluorometer (Thermo Fisher Scientific, Inc.). The library was then sequenced using HiSeq 2500 (Illumina, Inc.) (PE=125; data are available at DOI 10.4121/19086689). Data analysis was performed using the MAGeCK analysis (http://www.bioconductor.org/packages/release/bioc/html/MAGeCKFlute.html) (29). The sequencing was performed using a paired-end 125 (PE125) sequencing model. HRR efficiencies were evaluated according to the selective PCR results. Sequencing reads containing the selective PCR site and at least one variant in the donor library were used to calculate HRR efficiency.

Patients and clinical samples. A total of 772 breast cancer patients were admitted to the Affiliated Hospital of Hebei University (China) from August 2012 to September 2019. Among these, 538 patients (females; age range, 28 to 69 years; median age ± SD, 51.4±3.5 years) diagnosed with breast cancer were enrolled in this study. The study was approved by the Review Board of the Affiliated Hospital of Hebei University (approval number AHHU20200930). The inclusion criteria included the following: i) newly diagnosed cases; ii) *BRAC1/2* mutation detected; iii) completion of PAPRP inhibitor (olaparib) treatment and 5 years of follow-up. Information on patient treatment, recurrence, and survival status was well documented. Exclusion criteria included: i) recurrent breast cancer; ii) therapy performed prior to admission; and iii) comorbidities due to other clinical disorders. All patients were informed of the purpose of the experiment and signed informed consent. The clinical characteristics of the study subjects are shown in Table SII. Among the 538 patients who received the PARP inhibitor treatment, 68 were cases with a positive family history. The remaining 234 patients who failed to meet the inclusion criteria underwent surgical resection and adjuvant chemotherapy between August 2012 and September 2019. Of this group, those who did not receive PARP inhibitor treatment were also invited and accepted to participate as a population control. In the control group, the volunteers received standard medical and nursing care, such as vital sign observation, chemotherapy or surgical resection treatment and wound and pain management. Five patients withdrew voluntarily from follow-up in the next five years, but they agreed to our use of the data gathered during their follow-up.

Based on clinical findings, imaging information, histopathological tests, and other laboratory indicators, patients (cases) were graded according to the 8th edition AJCC standards (30). There were 70, 258, and 210 cases at clinical stages I, II, and III-IV, respectively. Patients were treated with surgical resection accompanied by chemotherapy. From the day of admission, all patients were followed for five years by telephone call or outpatient visits. Patients (n=2) who died from causes unrelated to breast cancer were excluded from the survival analysis.

Genotyping methods. DNA was extracted from all blood taken from the patients using a GenElut™ Blood Genomic DNA Kit

Table IV. Three haplotypes of *Rad51* WALKER domain in this study.

Haplotype	Alternative nuclei acids	Amino acids	Location (CDS)	Domain	Coefficient (95% CI)[a]
Haplotype-1	CC>AC; T>A	129L, 221E	387-388; 664	A and B	1.22
Haplotype-2	AA>GU	133V	397-398	A	0.83
Haplotype-3	GA>CC; UC>GU	128P, 129C	382-383; 386-387	A	0.75

[a]The logistic regression model (multivariate regression) indicates a significant interaction term showing that the effect of SNPs of WALKERA domain change with regard to the genotype of WALKERB domain, and vice versa. CDS, coding sequences; CI, confidence interval; SNPs, single nucleotide polymorphisms.

(Merck KGaA, Darmstadt, Germany). Five variants of *Rad51* (SNPs and repeat polymorphisms) (Table IV) were genotyped using SNAPshot (Thermo Fisher Scientific, Inc.).

Haplotype analysis. Haplotype frequencies of *Rad51* variants (five alternative amino acids listed in Table IV) were estimated using the Expectation-Maximization algorithm in the haplo.stats R software package (http://cran.r-project.org/web/packages/haplo.stats). The three assembled haplotypes were estimated separately in breast cancer patients at the above clinical stages. The R haplo.stats package was used to estimate the posterior probabilities of the haplotypes. The STATA haplologit command was used to model the association between haplotypes and case status as in a previous study (31).

Cell malignant behavior-related experiment

Cell Counting Kit-8 assay. The effects of cell transfections on cell proliferation were analyzed using a CCK-8 assay (Dojindo Laboratories, Inc.). A total of $5x10^3$ cells were seeded per well in 0.1 ml medium (containing 5 μM olaparib) in a 96-well cell culture plate. Three wells were set for each experiment. Cells were grown at 37˚C and collected at 24, 48, 72, and 96 h after the initiation of cell culture. The CCK-8 solution was added to each well to reach a final concentration of 10% at 4 h before harvesting cells. A microplate reader was used to read the OD values at 450 nm.

Colony formation assays. BT-549 cell suspension ($1x10^3$ cells per well) with/without the selected haplotype were obtained by trypsinization and filtration through a 40-μm filter, after which the cells were seeded in a 6-well plate (4,000 cells/well) containing 0.35% soft agar. The plates were then incubated in DMEM with 10% FBS for 1 day at 37˚C. Drug-containing medium (5 μM olaparib) was refreshed weekly. After two weeks, the cells were washed twice with PBS and fixed with methanol at 4˚C for 15 min, following which the colonies were stained with 0.1% crystal violet for 10 min at 25˚C.

Statistical analysis. All experiments were conducted in three technical replicates and three biological replicates, respectively. All data and survival curves were analyzed using GraphPad Prism (v.6) (GraphPad Software, Inc.) unless otherwise indicated. The quantitative data are presented as mean ± standard deviation (SD). All single nucleotide polymorphism strategies were employed to construct the haplotype. Haplotype analysis was performed using PHASE v2.1.1 software (31) and the frequencies of haplotypes were compared between all induced mutation cases vs. the wild-type. A logistic multivariate regression model was used to look for interactions between SNPs of the WALKER A domain and the genotype of WALKER B domain. Correlation analysis was carried out using Pearson's correlation coefficient. K-M plotter was used to plot survival curves, which were compared using a Mantel-Cox test. Log-rank test was performed to evaluate the hazard ratio (HR) and 95% confidence interval (CI). The non-parametric Mann-Whitney test was utilized for comparisons between two groups. For multiple groups, the Kruskal-Wallis test was utilized followed by Newman-Keuls test or Tukey's HSD. $P<0.05$ and $P<0.01$ were considered statistically significant and highly significant, respectively.

Results

sgRNA design and evaluation. In the pilot study, using flow cytometry we found that BT-549 cells displayed the highest sensitivity to olaparib (Fig. S1A and B). The sgRNAs, which were then designed according to the WALKER A and B domain-related PAM sequence, were scored using the CCTOP online prediction tool. The HDR library containing all possible missense mutations was constructed using a vector library containing a 7-bp selective PCR site mutation site at the PAM position and the selective PCR products were then identified by sequencing (Fig. 1A and B). The knockdown efficiencies for sgRNA1-1, sgRNA1-2, sgRNA2-1, sgRNA2-2, and sgRNA2-3 were 73.2, 54.9, 33.65, 68.05, and 71.4%, respectively; the off-target ratios were 1.03, 3.55, 2.71, 0.88, and 2.53%, respectively. The sgRNA-1-1 and sgRNA-2-2, which displayed relatively high knock-out efficiency and the lowest off-target ratios (73.2, 1.03; 68.05, and 0.88%, respectively) were then chosen for the subsequent experiments (Fig. 1C and D). Eight and five amino acids were found in the WALKER A and B domains, respectively. The saturated mutation of this region was obtained by residue substitutions of all 6,859 possible mutations (Fig. 1). Fig. 1C shows the selective PCR product region and evaluation of the off-target ratio.

Correlation between the induced mutagenesis on the target genomic region and the donor template. Fig. 2A shows that the frequency of the genomic region mutation was highly correlated with the donor template library. Five amino acid mutations (128P, 129C, 129L, 133V, and 221E) were associated with high resistance to olaparib at the amino acid

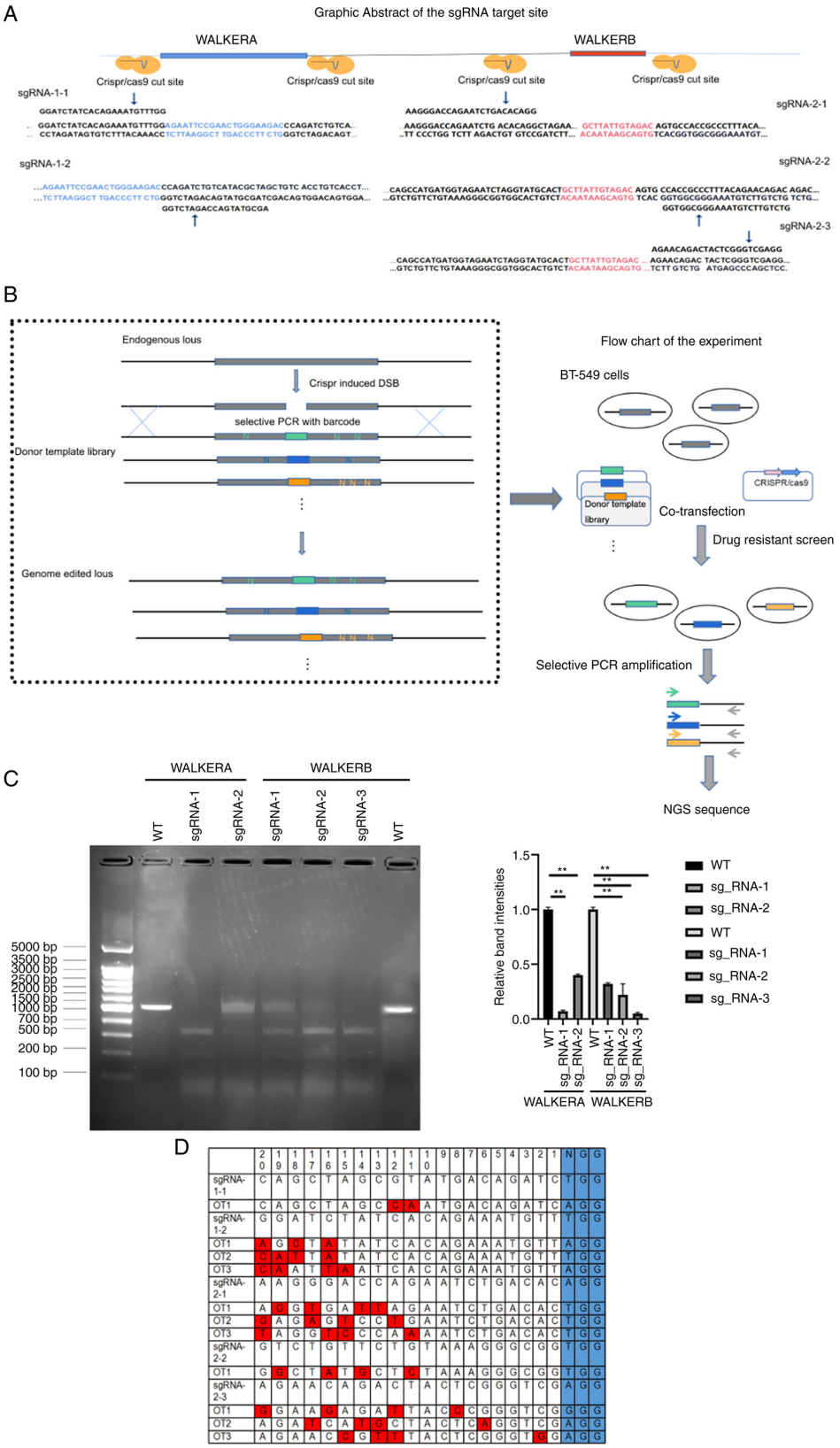

Figure 1. Overview of the CRISPR/Cas9-based *Rad51*-saturated mutagenesis system. (A) The three predicted sgRNAs targets in the *Rad51* WALKER A and B domains. The blue and red letters indicate the nucleic acid sequences for the WALKER A and B domains, respectively. The sgRNA was designed according to CCTP prediction which indicated the Cas9 cutting at the proper sites (arrow indicated). (B) The flow chart of the genome editing in the *Rad51* WALKER A and B domain. Co-transfection of CRISPR/Cas9 and homology-directed repair (HDR) donor template library in BT-549 cells. The half selective PCR sites were introduced into the donor template (color block), the other half primer sites were fixed in the homologous recombination repair (HRR) region. After co-transfection and drug screening, selective PCR was performed prior to sequencing to detect each single nucleotide variant (SNV) in the target region. (C) PCR products and measurement of the cleavage efficiencies of the MC3R targeting vectors using the T7E1 assay. The intensities of wild-type carriers were detected as reference values to which values of other carriers were normalized. The experiments were performed in triplicate and mean values were compared. Kruskal-Wallis test followed by Mann-Whitney test was used to compare the groups. **P<0.01. (D) The sequencing results of potential off-target sites. Nucleotides shown in red indicate the off-target sites. There were no off-target mutations in the *Rad51*-knockout (KO) cells.

Table V. Two-variant DAT haplotype frequency distributions.

	Control (n=234)			Treated with PARP inhibitors (n=538)		
Haplotype	Positive case	Negative case	Positive ratio (%)	Positive case	Negative case	Positve ratio (%)
Haplotype-1	113	121	48.3	345	193	64.1[a]
Haplotype-2	86	148	36.7	228	310	42.3[a]
Haplotype-3	23	211	9.8	92	446	17.1[a]

Three haplotypes were estimated using the Expectation-Maximization algorithm, stratified by drug resistance, then by case-control status. The positive ratio was compared to the control. Non-parametric Mann-Whitney test was performed to evaluate the statistical significance. [a]P<0.05.

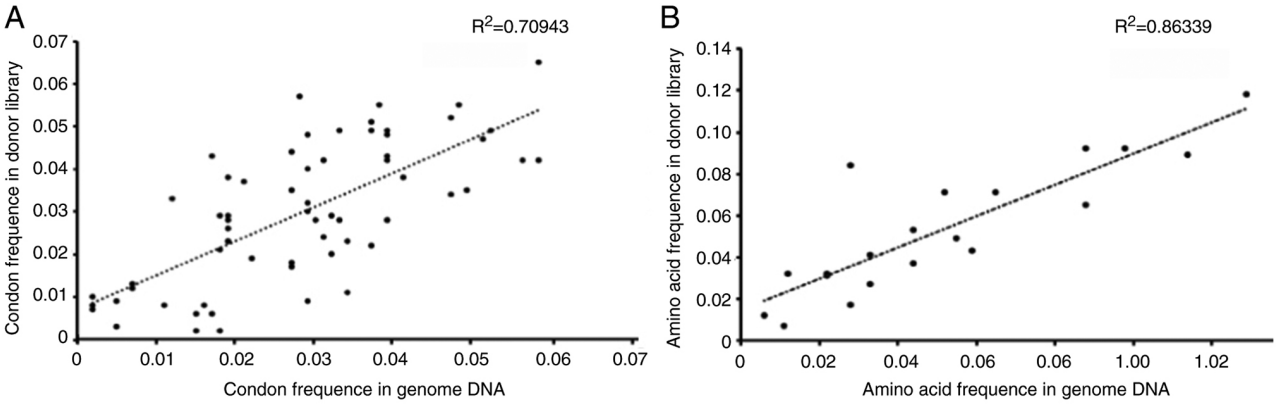

Figure 2. Comparison of the single nucleotide variant (SNV) editing rates in the genome and donor libraries. The correlation of the frequency of 64 triplet codons (A) and amino acids (B) between the donor library and editing region in the genome. Correlation analysis was carried out using Pearson's correlation coefficient (R^2=0.70943; R^2=0.86339, respectively). The plots indicate all 64 possible triplet codons (A), 20 amino acids and the stop codon (B), respectively.

level (Fig. 2B). The alternated wild-type amino acids for these residues are shown in Table IV. The missense mutation frequencies of the five alternative amino acids were determined. According to the targeted NGS results, these SNPs were also determined at the RNA level using RT-PCR. A good biomarker for clinical diagnosis should have high signal to noise ratio. Single missense mutations are rare and have low signal to noise ratio (32). Several contradictory studies for the association of *Rad51* genetic polymorphisms with cancer development have supported this viewpoint (33-35), although haplotyping can significantly overcome this drawback and improve the accuracy of the genetic polymorphisms (32,36). Therefore we assembled the SNPs into haplotypes using frequently co-occurring SNPs.

Haplotype assembly and effect. The following three haplotypes were assembled and identified in the olaparib-resistant cells (number indicates location of substitutions in cDNA): Haplotype 1 (387-388;664):CC>AC, T>A; Haplotype 2 (397-398):AA>GU; Haplotype 3 (382-383, 386-387):GA>CC, UC>GU (Fig. 2 and Table IV). Ten single clones were screened out by olaparib and evaluated by sequencing. All clones harbored at least one of the three haplotypes. Compared with the SNP results, it appeared that these haplotypes had greater discrimination ability in terms of cell survival, and cells with haplotype 2 and 3 showed the lowest sensitivity to olaparib (Fig. 3A and B) (P<0.05). Since RAD51 was a key HRR regulator which directly results in cell cycle arrest, we then investigated the effect of mutations in this gene on the cell proliferation and colony formation. The effects of haplotypes 1, 2 and 3 on the proliferation and cell viability of BT-549 cells were analyzed using the CCK-8 assay and colony formation assays. The former showed that harboring of the three haplotypes led to an increased proliferation of breast cancer cells (P<0.05) (Fig. 3C). In order to detect the tumorigenesis of tumor cells with/without the selected haplotype, colony formation assays was performed. Similarly, colony formation capacity was also enhanced in cells with the three haplotypes (Fig. 3D, P<0.05). Since the function of RAD51 is not directly related to apoptosis and cell migration, we did not investigate its effect on those cell behaviors. Furthermore, the cells were screened out in the olaparib-resistant experiment, indicating that the apoptosis ratio of this type of cell is very low and that the apoptosis difference would be difficult to determine

Association between haplotype and survival. The association between *Rad51* haplotypes and olaparib treatment was evaluated in 538 cases treated with PARP inhibitors and 234 controls (Table V). The distribution of the three *Rad51* haplotypes was predicted and identified among the patient samples. The results indicated that the positive ratio of the three haplotypes was significantly higher in the olaparib treatment group compared to the controls (Table V). Haplotypes 2 and 3 showed a lower positive ratio in both groups compared to haplotype 1. As

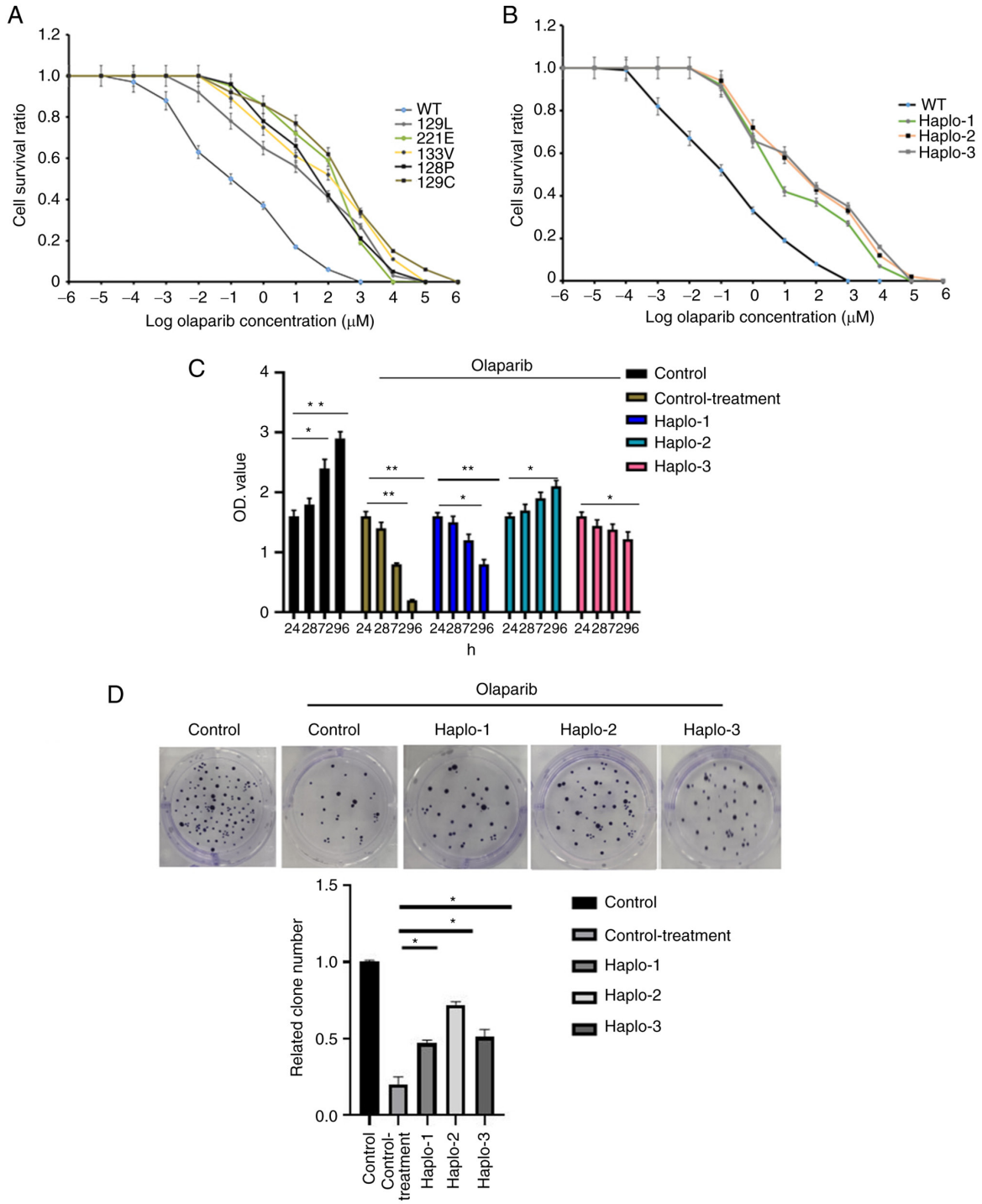

Figure 3. Olaparib resistance of *Rad51* mutants in BT-549 cells. (A) The survival analysis of BT-549 cells containing five amino acid mutations at increasing concentrations of olaparib. The mean IC_{50} values (μM) for wild-type, 129L, 221E, 133V, 128P and 129C were 0.61, 2.46, 2.8, 5.7 and 7.4 μM, respectively. One cell type originating from one single clone with triplicate repeats was analyzed. (B) The three haplotypes associated with olaparib resistance in BT-549 cells. The mean IC_{50} for wild-type, haplotype 1 (Haplo-1), haplotype 2 (Haplo-2), and haplotype 3 (Haplo-3) were 0.42, 1.74, 2.55, and 2.82 μM, respectively. Each x-axis indicates the Log drug concentration, and the y-axis indicates the survival rate. One cell type originating from one single clone with triplicate repeats was analyzed. The Kruskal-Wallis test was utilized followed by Newman-Keuls test to determine statistical significance. (C) The effects of haplotype 1 (Haplo-1), haplotype 2 (Haplo-2), and haplotype 3 (Haplo-3) carriers on cell proliferation were examined using the CCK-8 assay. The x-axis indicates the duration of olaparib treatment. (D) The colony formation capacities of BT-549 cells with haplotype 1 (Haplo-1), haplotype 2 (Haplo-2), and haplotype 3 (Haplo-3) were also analyzed. The olaparib concentration was 5 μM for both (C) and (D). All experiments were performed in triplicate and mean values were compared. Kruskal-Wallis test was utilized followed by Tukey's HSD to determine statistical significance. *P<0.05, **P<0.01.

shown in Fig. 3A and B, haplotypes 2 and 3 were likely more sensitive and specific to the resistance of PARP inhibitors. To further identify the potential drug resistance of haplotypes 1, 2 and 3 in clinical samples, we performed five-year survival analyses to compare 245 patient cases carrying any of these haplotypes (Fig. 4). Two haplotypes (haplotypes 2 and 3) were closely associated with breast cancer survival (HR=1.303, 95% CI=0.9922-1.711, for haplotype-2 VS control; HR=1.494,

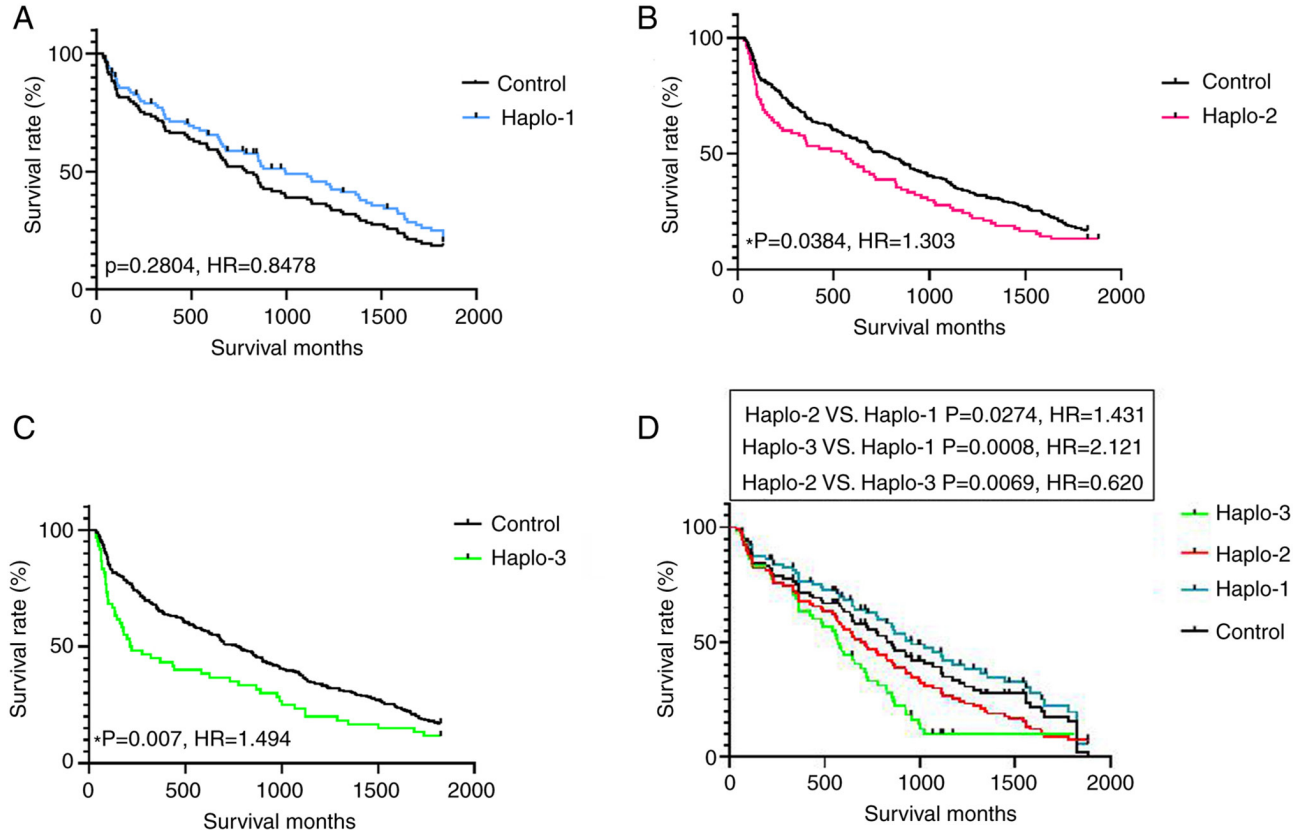

Figure 4. Two haplotypes are closely correlated with survival of breast cancer patients treated with olaparib. (A-C) Survival curves for patients with haplotype 1 (Haplo-1) (n=95), haplotype 2 (Haplo-2) (n=90) and haplotype 3 (Haplo-3) (n=60) and controls (n=230); (P=0.2804, P=0.0384 and P=0.007 respectively) (D) The combined survival curve for Haplo-1, Haplo-2, Haplo-3 and control. Haplo-2 vs. Haplo-1: P=0.0274, HR=1.431; Haplo-3 vs. Haplo-1: P=0.0008, HR=2.121; Haplo-2 vs. Haplo-3: P=0.0069, HR=0.620). The log-rank test was performed to determine the HR score and 95% confidence interval (CI). The Mantel-Cox test was performed to evaluate statistical significance. *P<0.05.

95% CI=1.063-2.100 for haplotype-3 VS control; HR=0.6197, 95% CI=0.4211–0.9120 for haplotype 2 VS haplotype 3). Haplotype-1 was not associated with survival (HR=0.8478, 95% CI=0.5848-1.077). The results indicated poorer prognosis with haplotype 3 than with haplotype 2 or 1.

Discussion

Several mechanisms have been proposed for the resistance to poly(ADP-ribose)polymerase (PARP) inhibitors. Many gene and protein mutations, as well as abnormal gene expression reportedly contribute to this cell function, including *Brca1/2* mutation, overexpression of *53bp1*, and increased drug transporter P-glycoprotein levels (37-39). RAD51 is central to three main double strand break repair pathways: gene conversion, synthesis-dependent strand annealing, and RAD51-dependent break-induced replication (40) and can enroll many other proteins to assemble RAD51 nuclear foci. According to previous research, the number of RAD51 nuclear foci is positively correlated with the resistance to PARP inhibitor (10), and the present findings confirm this correlation. A 10% cutoff point of the proportion of RAD51 nuclear foci score has previously been shown to predict the response to PARP inhibitors with high specificity and sensitivity (9). In the present study, the WALKER domain was the key structure in the homologous recombination repair (HRR) process. These results showed for the first time a saturation mutation genesis approach using targeted amino acid changes defined by single nucleotide mutations in this region adapted to explore the sensitivity to PARP inhibitors.

The CRISPR/Cas9-based system has the advantage of introducing random potential drug resistance mutations on a genome scale (41,42). Similarly, its role in saturation mutation screening is effective in loss-of-function screening using mammalian cells as well as animal models (16,17,43). We adopted this approach to identify olaparib resistance single nucleotide polymorphisms (SNPs) which are limited to a 13-amino acid window. Although the saturated mutation spectrum was random, the codon bias distribution was always selected for drug resistance (44,45). Next-generation sequencing (NGS) of selective PCR products from genomic DNA was used to identify functional mutation sites.

Our *in vitro* model experiments allowed us to observe the effects on cell proliferation to better understand the molecular evolution of drug resistance in breast cancers without *Brca1/2* mutations. Because RAD51 is a key HRR regulator which directly results in cell cycle arrest, we investigated the effect of mutations in this gene on the cell proliferation and colony formation. After selecting clones exposed to olaparib, cells with fit mutations remained viable. Our findings showed that a single nucleotide mutation achieved similar effects on cell survival as the combination of multiple nucleotide mutations. Multiple nucleotide substitutions as a group appeared to have a stronger capacity to distinguish mutations from wild-type codons in drug

resistance during the evaluation of olaparib resistance in *Rad51*. Haplotype assembly was used to identify the possible combined effect of these SNPs. Three haplotypes were assembled and drug resistance was assessed at the cell level. To evaluate the clinical value of these haplotypes, a series of clinical samples were screened to identify the potential predictive ability of the mutational pathway. The frequency distributions of these haplotypes were also investigated in all the clinical subjects (Table V), and they were also observed in control cohorts suggesting that they may be natural variations which were enriched after PARP treatment. Finally, two haplotypes were selected as potential prognostic biomarkers for olaparib resistance in patients with breast cancer chemoresistance.

The mutations found to cause drug resistance in patients are often not clear until drugs are used clinically. Multi-drug resistance is frequently observed during cancer treatment with a PARP inhibitor (46,47) and the related pathways involve several genes, each of which always contains several mutations (48). Mutations are highly variable and are strongly influenced by sex, race, ethnicity, and even individual differences (49,50). Furthermore, some functional mutations frequently co-occur with other underlying mutations making it difficult to screen and accurately identify valuable drug-resistant mutations for a specific drug (51). In recent years, the CRISPR/Cas9-based negative screening strategy with high-throughput random screening has been applied to identify potential drug resistance mutations. Due to the limits of library construction, the induced mutation is identified within a limited region of the gene sequence, while randomly induced mutations are rarely observed in clinical samples and have limited clinical validity (52-54). The CRISPR/Cas9-based saturation mutation strategy to identify the drug resistance pathway hub gene displays high efficiency and clinical utility. It may provide a new approach to identify clinically useful mutations from *in vitro* studies. Finally, to improve the 'resolving power' of the induced mutations, we assembled mutations according to haplotype and evaluated these haplotypes in clinical samples. Two haplotypes (haplotypes-2 and -3) were identified as prognostic markers for breast cancer with olaparib treatment.

Compared to traditional methods, the targets identified using this method have been determined with high efficiency and low cost. Given the limits of the editing efficiency and individual differences, the single mutation site randomly induced by the CRISPR/Cas9 system is rarely used to evaluate the response to drug treatment and lacks clinical value. Therefore, a saturation mutagenesis method for specific oncogene or tumor suppressor genes seems more efficient to screen for valuable mutations. The bottleneck of this method is the paradox between the limited content of the donor library and the number of targets. Improvement of the payload information stored in the donor library and the efficiency of the genome editing may be key to resolving this issue. The present study was also limited by the size and lack of diversity of the sample, restricting the clinical applicability of the findings. The explored markers therefore need to be verified in a larger and more diverse clinical cohort. Overall, the results of our study provide a new strategy to identify functional drug resistance mutations.

In conclusion, the present study assessed a series of saturated mutations of the *Rad51* WALKER domain induced using a CRISPR/Cas9-based approach. Five SNPs were screened and were associated with the response to olaparib treatment. Finally, two haplotypes were assembled and evaluated in clinical samples. Haplotypes 2 and 3 were associated with breast cancer survival and provide a potential hallmark for breast cancer chemoresistance to PARP inhibitor. The patients with these haplotypes may have relatively poor prognosis.

Acknowledgements

Not applicable.

Funding

This work was supported by the Scientific Research Fund of the Affiliated Hospital of Hebei University (China) (no. 8207102536).

Availability of data and materials

The analyzed data sets generated during the study are available from the corresponding author on reasonable request.

Authors' contributions

HY, XL and LR designed the present study. HY, YW and QZ conducted the experiments. YY and XL conducted the experiments and the statistical analysis. XB and LY analyzed and interpreted the patient data. NX interpreted the results. HY wrote the manuscript. AZ was involed in drafting and revising the manuscript and also contributed to analysis and interpretation of halpotype assemble data. XL was involved in designing and drafting the framework of the study. XL was also responsible for the layout of the figures. XL and LR revised the final version and confirm the authenticity of all the raw data. All authors read and approved the final manuscript for publication.

Ethics approval and consent to participate

The authors obtained appropriate institutional review board approval from the Ethics Committee of the Affiliated Hospital of Hebei University (Hebei, China) (no. AHHU20200930). Informed consent was obtained from the participants involved.

Patient consent for publication

The authors confirm that they have obtained written consent from each patient to publish the manuscript.

Competing interests

The authors declare that they have no competing interests.

References

1. Mavaddat N, Antoniou AC, Easton DF and Garcia-Closas M: Genetic susceptibility to breast cancer. Mol Oncol 4: 174-191, 2010.
2. Lord CJ and Ashworth A: BRCAness revisited. Nat Rev Cancer 16: 110-120, 2016.
3. Apostolou P and Fostira F: Hereditary breast cancer: The era of new susceptibility genes. Biomed Res Int 2013: 747318, 2013.

4. Noordermeer SM and van Attikum H: PARP Inhibitor Resistance: A tug-of-war in BRCA-mutated cells. Trends Cell Biol 29: 820-834, 2019.
5. Risdon EN, Chau CH, Price DK, Sartor O and Figg WD: PARP Inhibitors and prostate cancer: To infinity and beyond BRCA. Oncologist 26: e115-e129, 2021.
6. Bajrami I, Frankum JR, Konde A, Miller RE, Rehman FL, Brough R, Campbell J, Sims D, Rafiq R, Hooper S, *et al*: Genome-wide profiling of genetic synthetic lethality identifies CDK12 as a novel determinant of PARP1/2 inhibitor sensitivity. Cancer Res 74: 287-297, 2014.
7. Grundy MK, Buckanovich RJ and Bernstein KA: Regulation and pharmacological targeting of RAD51 in cancer. NAR Cancer 2: zcaa024, 2020.
8. Kolinjivadi AM, Sannino V, de Antoni A, Técher H, Baldi G and Costanzo V: Moonlighting at replication forks-a new life for homologous recombination proteins BRCA1, BRCA2 and RAD51. FEBS Lett 591: 1083-1100, 2017.
9. Cruz C, Castroviejo-Bermejo M, Gutiérrez-Enríquez S, Llop-Guevara A, Ibrahim YH, Gris-Oliver A, Bonache S, Morancho B, Bruna A, Rueda OM, *et al*: RAD51 foci as a functional biomarker of homologous recombination repair and PARP inhibitor resistance in germline BRCA-mutated breast cancer. Ann Oncol 29: 1203-1210, 2018.
10. Castroviejo-Bermejo M, Cruz C, Llop-Guevara A, Gutiérrez-Enríquez S, Ducy M, Ibrahim YH, Gris-Oliver A, Pellegrino B, Bruna A, Guzmán M, *et al*: A RAD51 assay feasible in routine tumor samples calls PARP inhibitor response beyond BRCA mutation. EMBO Mol Med 10: e9172, 2018.
11. Malka MM, Eberle J, Niedermayer K, Zlotos DP and Wiesmüller L: Dual PARP and RAD51 inhibitory drug conjugates show synergistic and selective effects on breast cancer cells. Biomolecules 11: 981, 2021.
12. Moudry P, Watanabe K, Wolanin KM, Bartkova J, Wassing IE, Watanabe S, Strauss R, Troelsgaard Pedersen R, Oestergaard VH, Lisby M, *et al*: TOPBP1 regulates RAD51 phosphorylation and chromatin loading and determines PARP inhibitor sensitivity. J Cell Biol 212: 281-288, 2016.
13. Garcin EB, Gon S, Sullivan MR, Brunette GJ, Cian A, Concordet JP, Giovannangeli C, Dirks WG, Eberth S, Bernstein KA, *et al*: Differential requirements for the Rad51 paralogs in genome repair and maintenance in human cells. PLoS Genet 15: e1008355, 2019.
14. Abreu CM, Prakash R, Romanienko PJ, Roig I, Keeney S and Jasin M: Shu complex SWS1-SWSAP1 promotes early steps in mouse meiotic recombination. Nat Commun 9: 3961, 2018.
15. Fang P, De Souza C, Minn K and Chien J: Genome-scale CRISPR knockout screen identifies TIGAR as a modifier of PARP inhibitor sensitivity. Commun Biol 2: 335, 2019.
16. Ma L, Boucher JI, Paulsen J, Matuszewski S, Eide CA, Ou J, Eickelberg G, Press RD, Zhu LJ, Druker BJ, *et al*: CRISPR-Cas9-mediated saturated mutagenesis screen predicts clinical drug resistance with improved accuracy. Proc Natl Acad Sci USA 114: 11751-11756, 2017.
17. Findlay GM, Boyle EA, Hause RJ, Klein JC and Shendure J: Saturation editing of genomic regions by multiplex homology-directed repair. Nature 513: 120-123, 2014.
18. Burger A, Lindsay H, Felker A, Hess C, Anders C, Chiavacci E, Zaugg J, Weber LM, Catena R, Jinek M, *et al*: Maximizing mutagenesis with solubilized CRISPR-Cas9 ribonucleoprotein complexes. Development 143: 2025-2037, 2016.
19. Pelttari LM, Kiiski JI, Ranta S, Vilske S, Blomqvist C, Aittomäki K and Nevanlinna H: RAD51, XRCC3, and XRCC2 mutation screening in Finnish breast cancer families. Springerplus 4: 92, 2015.
20. Short JM, Liu Y, Chen S, Soni N, Madhusudhan MS, Shivji MK and Venkitaraman AR: High-resolution structure of the presynaptic RAD51 filament on single-stranded DNA by electron cryo-microscopy. Nucleic Acids Res 44: 9017-9030, 2016.
21. Xu J, Zhao L, Xu Y, Zhao W, Sung P and Wang HW: Cryo-EM structures of human RAD51 recombinase filaments during catalysis of DNA-strand exchange. Nat Struct Mol Biol 24: 40-46, 2017.
22. Chen J, Villanueva N, Rould MA and Morrical SW: Insights into the mechanism of RAD51 recombinase from the structure and properties of a filament interface mutant. Nucleic Acids Res 38: 4889-4906, 2010.
23. Bonilla B, Hengel SR, Grundy MK and Bernstein KA: Rad51 gene family structure and function. Annu Rev Genet 54: 25-46, 2020.
24. Baldock RA, Pressimone CA, Baird JM, Khodakov A, Luong TT, Grundy MK, Smith CM, Karpenshif Y, Bratton-Palmer DS, Prakash R, *et al*: Rad51D splice variants and cancer-associated mutations reveal XRCC2 interaction to be critical for homologous recombination. DNA Repair (Amst) 76: 99-107, 2019.
25. Corrales-Sánchez V, Noblejas-López MDM, Nieto-Jiménez C, Pérez-Peña J, Montero JC, Burgos M, Galán-Moya EM, Pandiella A and Ocaña A: Pharmacological screening and transcriptomic functional analyses identify a synergistic interaction between dasatinib and olaparib in triple-negative breast cancer. J Cell Mol Med 24: 3117-3127, 2020.
26. Stemmer M, Thumberger T, Del Sol Keyer M, Wittbrodt J and Mateo JL: CCTop: An intuitive, flexible and reliable CRISPR/Cas9 target prediction tool. PloS One 10: e0124633, 2015.
27. Kamel D, Gray C, Walia JS and Kumar V: PARP inhibitor drugs in the treatment of breast, ovarian, prostate and pancreatic cancers: An update of clinical trials. Curr Drug Targets 19: 21-37, 2018.
28. Chu CY, Lee YC, Hsieh CH, Yeh CT, Chao TY, Chen PH, Lin IH, Hsieh TH, Shih JW, Cheng CH, *et al*: Genome-wide CRISPR/Cas9 knockout screening uncovers a novel inflammatory pathway critical for resistance to arginine-deprivation therapy. Theranostics 11: 3624-3641, 2021.
29. Wang B, Wang M, Zhang W, Xiao T, Chen CH, Wu A, Wu F, Traugh N, Wang X, Li Z, *et al*: Integrative analysis of pooled CRISPR genetic screens using MAGeCKFlute. Nat Prot 14: 756-780, 2019.
30. Giuliano AE, Edge SB and Hortobagyi GN: Eighth edition of the AJCC cancer staging manual: Breast cancer. Ann Surg Oncol 25: 1783-1785, 2018.
31. Shen B, Zhang J, Wu H, Wang J, Ma K, Li Z, Zhang X, Zhang P and Huang X: Generation of gene modified mice via Cas9/RNA-mediated gene targeting. Cell Res 23: 720-723, 2013.
32. Stephens M and Scheet P: Accounting for decay of linkage disequilibrium in haplotype inference and missing-data imputation. Am J Hum Genet 76: 449-462, 2005.
33. Li P, Guo M, Wang C, Liu X and Zou Q: An overview of SNP interactions in genome-wide association studies. Brief Funct Genomics 2: 143-155, 2015.
34. Tulbah S, Alabdulkarim H, Alanazi M, Parine NR, Shaik J, Pathan AA, Al-Amri A, Khan W and Warsy A: Polymorphisms in Rad51 and their relation with breast cancer in Saudi females. Onco Targets 9: 269-277, 2016.
35. Vral A, Willems P, Claes K, Poppe B, Perletti G and Thierens H: Combined effect of polymorphisms in Rad51 and Xrcc3 on breast cancer risk and chromosomal radiosensitivity. Mol Med Rep 4: 901-912, 2011.
36. Brooks J, Shore RE, Zeleniuch-Jacquotte A, Currie D, Afanasyeva Y, Koenig KL, Arslan AA, Toniolo P and Wirgin I: Polymorphisms in RAD51, XRCC2, and XRCC3 are not related to breast cancer risk. Cancer Epidemiol Biomark Prev 17: 1016-1019, 2008.
37. Kim JH and Hong YC: Modification of PARP4, XRCC3, and RAD51 gene polymorphisms on the relation between Bisphenol A exposure and liver abnormality. Int J Environ Res Public Health 17: 2794, 2020.
38. Marchenko YV, Carroll RJ, Lin DY, Amos CI and Gutierrez RG: Semiparametric analysis of case-control genetic data in the presence of environmental factors. Stata J 8: 305-333, 2008.
39. Hurley RM, Wahner Hendrickson AE, Visscher DW, Ansell P, Harrell MI, Wagner JM, Negron V, Goergen KM, Maurer MJ, Oberg AL, *et al*: 53BP1 as a potential predictor of response in PARP inhibitor-treated homologous recombination-deficient ovarian cancer. Gynecol Oncol 153: 127-134, 2019.
40. Nacson J, Krais JJ, Bernhardy AJ, Clausen E, Feng W, Wang Y, Nicolas E, Cai KQ, Tricarico R, Hua X, *et al*: Brca1 mutation-specific responses to 53bp1 loss-induced homologous recombination and PARP inhibitor resistance. Cell Rep 24: 3513-3527. e7, 2018.
41. Jaspers JE, Kersbergen A, Boon U, Sol W, van Deemter L, Zander SA, Drost R, Wientjens E, Ji J, Aly A, *et al*: Loss of 53BP1 causes PARP inhibitor resistance in Brca1-mutated mouse mammary tumors. Cancer Discov 3: 68-81, 2013.
42. Symington LS and Gautier J: Double-strand break end resection and repair pathway choice. Annu Rev Genet 45: 247-271, 2011.
43. Shalem O, Sanjana NE, Hartenian E, Shi X, Scott DA, Mikkelson T, Heckl D, Ebert BL, Root DE, Doench JG and Zhang F: Genome-scale CRISPR-Cas9 knockout screening in human cells. Science 343: 84-87, 2014.
44. Koike-Yusa H, Li Y, Tan EP, Velasco-Herrera Mdel C and Yusa K: Genome-wide recessive genetic screening in mammalian cells with a lentiviral CRISPR-guide RNA library. Nat Biotechnol 32: 267-273, 2014.

45. Yamauchi T, Masuda T, Canver MC, Seiler M, Semba Y, Shboul M, Al-Raqad M, Maeda M, Schoonenberg VAC, Cole MA, *et al*: Genome-wide CRISPR-Cas9 screen identifies leukemia-specific dependence on a Pre-mRNA metabolic pathway regulated by DCPS. Cancer Cell 33: 386-400. e5, 2018.
46. Ali M, Kaltenbrun E, Anderson GR, Stephens SJ, Arena S, Bardelli A, Counter CM and Wood KC: Codon bias imposes a targetable limitation on KRAS-driven therapeutic resistance. Nat Commun 8: 15617, 2017.
47. Morio F, Lombardi L and Butler G: The CRISPR toolbox in medical mycology: State of the art and perspectives. PLoS Pathog 16: e1008201, 2020.
48. Gout J, Perkhofer L, Morawe M, Arnold F, Ihle M, Biber S, Lange S, Roger E, Kraus JM, Stifter K, *et al*: Synergistic targeting and resistance to PARP inhibition in DNA damage repair-deficient pancreatic cancer. Gut 70: 743-760, 2021.
49. Dallavalle S, Dobričić V, Lazzarato L, Gazzano E, Machuqueiro M, Pajeva I, Tsakovska I, Zidar N and Fruttero R: Improvement of conventional anti-cancer drugs as new tools against multidrug resistant tumors. Drug Resist Update 50: 100682, 2020.
50. Laucht M, Skowronek MH, Becker K, Schmidt MH, Esser G, Schulze TG and Rietschel M: Interacting effects of the dopamine transporter gene and psychosocial adversity on attention-deficit/hyperactivity disorder symptoms among 15-year-olds from a high-risk community sample. Arch Gen Psychiatry 64: 585-590, 2007.
51. Caspi A, Sugden K, Moffitt TE, Taylor A, Craig IW, Harrington H, McClay J, Mill J, Martin J, Braithwaite A and Poulton R: Influence of life stress on depression: Moderation by a polymorphism in the 5-HTT gene. Science 301: 386-389, 2003.
52. Aguiar D, Wong WS and Istrail S: Tumor haplotype assembly algorithms for cancer genomics. Pac Symp Biocomput: 3-14, 2014.
53. Azam M, Latek RR and Daley GQ: Mechanisms of autoinhibition and STI-571/imatinib resistance revealed by mutagenesis of BCR-ABL. Cell 112: 831-843, 2003.
54. Ma Y, Zhang J, Yin W, Zhang Z, Song Y and Chang X: Targeted AID-mediated mutagenesis (TAM) enables efficient genomic diversification in mammalian cells. Nat Methods 13: 1029-1035, 2016.